13. V.Elser, Phys.Rev.B32, 4892 (1985).
14. R.K.P.Zia and W.J.Dallas, J.Phys.A18, L341 (1985).
15. V.Hoggatt, Fibonacci and Lucas Numbers (Houghton Mifflin Co., Boston, 1969).
16. S.Tamura and J.P.Wolfe, Phys.Rev.B36, 3491 (1987).
17. J.P.Lu, T.Odagaki and J.L.Birman, Phys.Rev.B33, 4809 (1986).
18. M.Kohmoto and J.R.Banavar, Phys.Rev.B34, 563 (1986).
19. F.Nori and J.P.Rodriguez, Phys.Rev.B34, 2207 (1986).
20. X.K.Zhang, H.Xia, G.X.Cheng, A.Hu and D.Feng, Phys.Lett.A136, 312 (1989).
21. H.R.Ma and C.H.Tsai, Phys.Rev.B35, 9295 (1987).
22. L.X.Zhang, Y.Y.Zhu, and N.B.Ming, (submitted).
23. V.M.Ristic, in 1972 IEEE Ultrasonics Symposium, edited by J.DeKlerk, p424.
24. Y.Y.Zhu, N.B.Ming, W.H.Jiang and Y.A.Shui, Appl.Phys.Lett.53, 1381 (1988).
25. Y.Y.Zhu, N.B.Ming, W.H.Jiang and Y.A.Shui, Appl.Phys.Lett.53, 2278 (1988).

CHAPTER 4

Nonlinear optic effect of quasiperiodic optic superlattice

Since the discovery of the quasicrystal,many researches were directed toward its linear phenomena[1-3] and its third-order nonlinearity[4,5].Little has been done on the second-order nonlinear optical phenomena because of lack of proper materials.

The Fibonacci optic superlattice(FOS) provides a useful tool for the study of such phenomena.

In this chapter,we will first study the spectrum of the second harmonic of the FOS[6]. Then we will study the harmonic generations and propose the phase-matching concept for the FOS[7]. By a more rigorous theoretical treatment,one backward-going second harmonic has been predicted.

PART 1

Second harmonic spectrum[6]

There are many theoretical and experimental studies which have shown that the spectra of the quasicrystal, such as those of x-ray diffraction[4], phonon[1,2,8,9], electronic energy structure[1] and polariton[10] etc., are all self-similar. Here we report our theoretical results of the spectrum of the second harmonic in an FOS[6]. Owing to the dispersive effect of the refractive index, the spectrum does not possess the self-similarity. And by an adequate choice of the structure parameters, an extinction phenomenon is found.

§4—1—1. Theory

The FOS used here is shown in Fig.1—3. Here we have set $t=\tau=\frac{1}{2}(1+\sqrt{5})$ and retained only two adjustable parameters l and η. Through the variation of the value of η, the structure can be either a periodic superlattice or a quasiperiodic one. For example, if $\eta=0$, then the structure is a periodic one, otherwise it is a quasiperiodic one. In our system, l and η play an important role, so we call them structure parameters.

As will be seen below, the phase-matching regime can not be used to study the effect of the FOS on the nonlinear optical phenomena. So the quasi-phase-matching concept[11,12] should be developed. In order to use the largest nonlinear optical coefficient d_{33} of $LiNbO_3$ crystals, we assume that the domain boundaries are parallel to the yz plane(Fig.1—3) and that the polarization of the electric fields are along the z axis with their propagating directions along the x axis.

In what follows, we will limit ourselves to the case of the second harmonic generation (SHG) with a single laser beam incident onto the surface of the FOS. Starting from the Maxwell equation[13,14].

$$\nabla^2\vec{E}(x,t)-\frac{\varepsilon_3}{c^2}\frac{\partial^2\vec{E}(x,t)}{\partial t^2}=\frac{4\pi}{c^2}\frac{\partial^2\vec{P}(x,t)}{\partial t^2}, \qquad (4—1—1)$$

and using the small signal approximation, we get

$$\frac{d^2E_2}{dx^2} - 2ik^{2\omega}\frac{dE_2}{dx} = -\frac{32\pi\omega^2}{c^2} d_{33} f(x) E_1^2 e^{i(k^{2\omega}-2k^{\omega})x} . \quad (4—1—2)$$

with E_2 taking the form

$$E_2(x,t) = E_2(x) e^{i(2\omega t - k^{2\omega}x)} . \quad (4—1—3)$$

Where, ω and k^{ω} are the angular frequency and wave number of the fundamental beam respectively, $k^{2\omega}$ is the wave number of the second harmonic and c is the light speed in vacuum, $\vec{P}$ is the nonlinear polarization vector.

Conventionally, the second-order derivative in Eq.(4—1—2) is neglected which is the so-called parabolic approximation. Eq.(4—1—2) turns into

$$\frac{dE_2}{dx} = -i\frac{16\pi\omega^2}{k^{2\omega}c^2} d_{33} f(x) E_1^2 e^{i(k^{2\omega}-2k^{\omega})x} . \quad (4—1—4)$$

By integrating Eq.(4—1—4), the second harmonic electric field after passing through N blocks of the FOS can be represented as

$$E_2(N) = -\frac{32\pi\omega^2}{k^{2\omega}c^2\Delta k} d_{33} E_1^2 \left\{ \sum_{n=2j+1} e^{i\Delta k x_n} + e^{i\pi} \sum_{n=2j} e^{i\Delta k x_n} \right\}, \quad (4—1—5)$$

where $\Delta k = k^{2\omega} - 2k^{\omega}$ and j=0, 1, 2, ... $\{x_n\}$ are the positions of the ferroelectric domain boundaries(Fig.1—3).

In Eq.(4—1—5), the terms inside the braces are the structure factor which is divided into two parts with one

part lagging behind the other a phase of exp[i($\Delta kl+\pi$)].

For an infinite array with $l_A/l_B=\tau$ (i.e., $\eta=0.34$), by use of direct[15] or projection[16] method, Eq.(4—1—5) can be written in the form

$$E_2(\Delta k)=-i\frac{32\pi\omega^2}{k^2\omega_c^2}d_{33}E_1^2\sum_{m,n}e^{i(\frac{1}{2}G_{m,n}l-X_{m,n})}\frac{\sin\frac{1}{2}G_{m,n}l}{\frac{1}{2}G_{m,n}}\cdot\frac{\sin X_{m,n}}{X_{m,n}}$$

$$\times\delta(\Delta k-G_{m,n}). \qquad (4—1—6)$$

By using Eq.(1—21) and integrating Eq.(4—1—4) directly, E_2 can also be expressed as

$$E_2(N)=-i\frac{32\pi\omega^2}{k^2\omega_c^2}d_{33}E_1^2\sum_{m,n}e^{i(\frac{1}{2}G_{m,n}l-X_{m,n})}\frac{\sin\frac{1}{2}G_{m,n}l}{\frac{1}{2}G_{m,n}}\cdot\frac{\sin X_{m,n}}{X_{m,n}}$$

$$\times\frac{\sin(\Delta k-G_{m,n})X_N}{\pi(\Delta k-G_{m,n})}. \qquad (4—1—7)$$

Where $\Delta k=k^{2\omega}-2k^{\omega}$.

According to the definetion of the delta function

$$\delta(k)=\lim_{N\to\infty}\frac{1}{2\pi}\int_{-X_N}^{X_N}e^{iku}du, \qquad (4—1—8)$$

these two results are the same.

For a periodic optic superlattice, a similar expression can be obtained which is

$$E_2(\Delta k)=-i\frac{32\pi\omega^2}{k^2\omega_c^2}d_{33}E_1^2\sum_{m\neq 0}\frac{i(1-\cos m\pi)}{m\pi}e^{i\frac{1}{2}G_m l}\sin\frac{1}{2}G_m l$$

$$\times\frac{\sin(\Delta k-G_m)X_N}{(\Delta k-G_m)}, \qquad (4\text{—}1\text{—}9)$$

where G_m is the reciprocal vector of the periodic structure, l is the thickness of the positive domain.

The appearance of Δk is due to the energy coupling between the fundamental beam and the second harmonic through the nonlinear optical effect. Obviously the FOS can not be used to the study of the SHG with phase matched ($\Delta k=0$). It can be only used to the study of the SHG with quasi-phase-matchable.

§4—1—2. Spectrum of the second harmonic

The peaks of the second harmonic intensity can be obtained from the δ-function in Eq.(4—1—6), which is

$$\Delta k_{m,n}=\frac{2\pi(m+n\tau)}{D}, \qquad (4\text{—}1\text{—}10)$$

or

$$(\Delta kD)_{m,n}=2\pi(m+n\tau). \qquad (4\text{—}1\text{—}11)$$

From Eq.(4—1—11) we will discuss some interesting phenomena in both real space and reciprocal space. All calculation results are valid only under room temperature and without the loss of generality, only the results with

N=100 have been presented.

In real space, we study the dependence of the second harmonic intensity on the structure parameter l of the FOS. In this case, the wave length λ_0 is kept unchanged, so are the refractive indices n_{10} and n_{20}. Here λ_0 represents the wavelength of the fundamental frequency in vacuum, n_{10} and n_{20} are the refractive indices for the fundamental beam and the second harmonic, respectively. Thus the dispersion of the refractive indices has no effect on the second harmonic spectrum. Eq.(4—1—11) can be rewritten as

$$l_{m,n}=\frac{(m+n\tau)\lambda_0}{4(n_{20}-n_{10})(1+\tau)} \qquad (4—1—12)$$

For those intense peaks, Eq.(4—1—12) becomes

$$I(s,p)=\frac{\lambda_0}{4(n_{20}-n_{10})(1+\tau)}\, s\tau^p, \qquad (4—1—13)$$

here s and p are integers.

Obviously here the relation $I(s,p+1)=I(s,p)+I(s,p-1)$ holds and thus the spectrum of the second harmonic exhibits self-similarity. Fig.4—1—1 shows the relation between the second harmonic intensity and the structure parameter l with the pump beam at wave length $\lambda_0=1.318\mu m$ and $n_{10}=2.1453$, $n_{20}=2.1970$ for $LiNbO_3$ crystals under the condition $l_A/l_B=\tau$. The result conforms with the discussion above. The intense peaks take the form of $\lambda_0 s\tau^p/[4(n_{20}-n_{10})(1+\tau)]$. Under general conditions, i.e., $l_A\neq\tau l_B$, calculations have shown that the peak positions of the second harmonic intensity

keep unchanged except their strengths.In our case, the change of the value of τ does not affect the value of D. This can be seen easily from the relation $D=\tau l_A+l_B=2l(1+\tau)$. This indicates that D is a characteristic parameter of the FOS. The result is consistent with that of R.Merlin et al[4]. They found that for all $l_A \neq l_B$, the Fourier spectrum of the structure factor of a Fibonacci superlattice consists of δ-function peaks at $k=2\pi(m+n\tau)/D$ with $D=\tau l_A+l_B$. We may deduce from these results that the FOS possess certain space

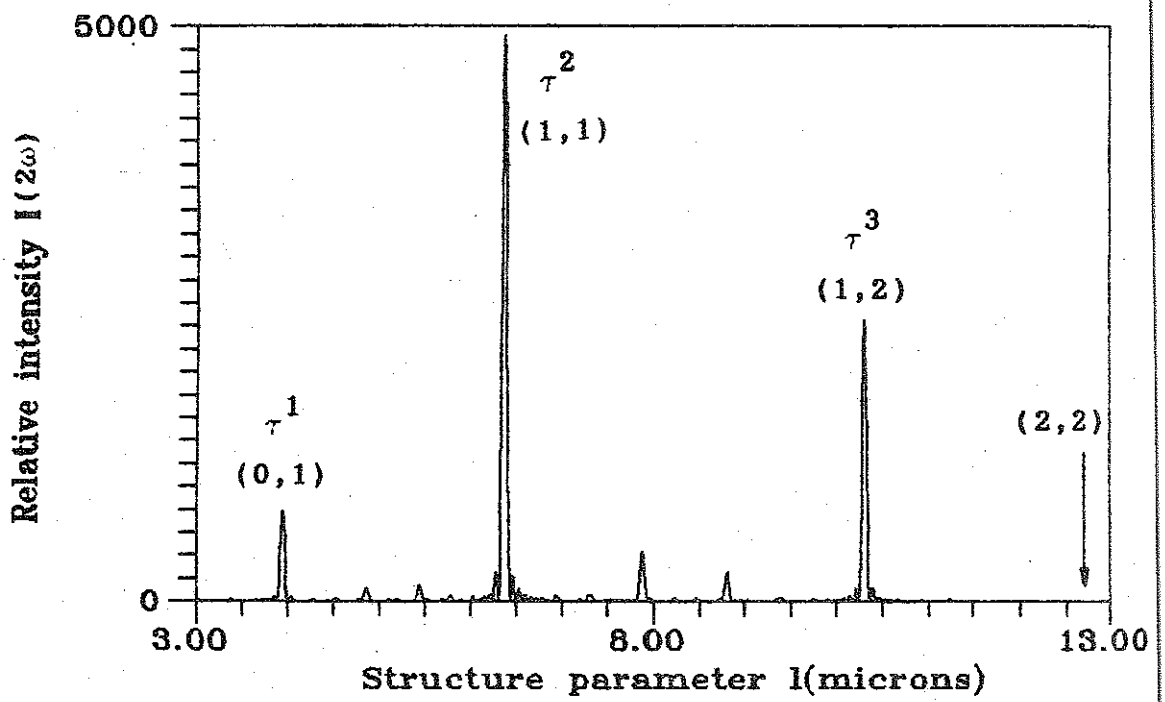

Fig.4—1—1.Dependence of the second harmonic intensity on the structure parameter l in real space.Note that $I(s,p+1)=I(s,p)+I(s,p-1)$.

symmetry. The symmetry is determined by the arrangement order of the blocks not by the block thicknesses.

In reciprocal space, we study the dependence of the second harmonic intensity on the wave length λ. In this case, the structure parameter l is kept constant. Eq.(4—1—11) can be rewritten as

$$\left(\frac{1}{\lambda}\right)_{m,n}=\frac{m+n\tau}{4[n_2(\lambda)-n_1(\lambda)](1+\tau)l}\ , \qquad (4—1—14)$$

here $n_1(\lambda)$ and $n_2(\lambda)$ are functions of λ[17]. Eq.(4—1—14) indicates here the dispersive effect of the refractive index on the second harmonic spectrum must be taken into account. Though, for those intense peaks, Eq.(4—1—14) becomes

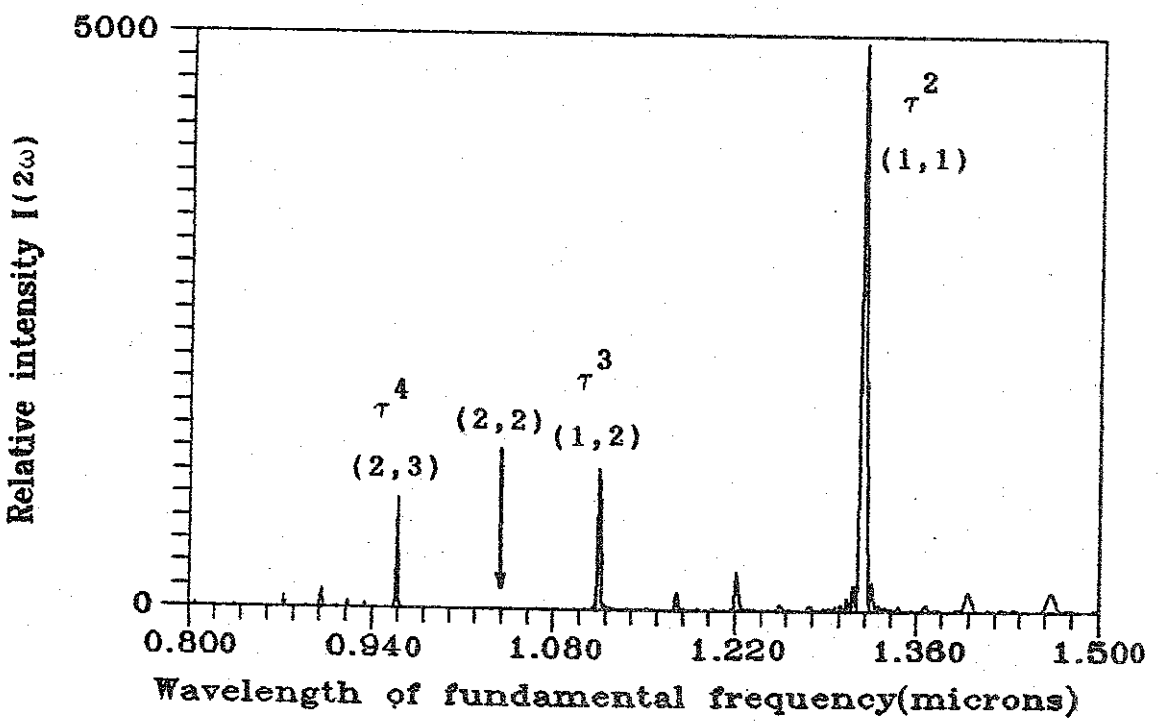

Fig.4—1—2.Dependence of the second harmonic intensity on the fundamental wavelength in reciprocal space. Note that $(1/\lambda)_{s,p+1}\neq(1/\lambda)_{s,p}+(1/\lambda)_{s,p-1}$.

$$(\frac{1}{\lambda})_{s,p}=\frac{s\tau^{p}}{4[n_2(\lambda)-n_1(\lambda)](1+\tau)l}, \qquad (4\text{—}1\text{—}15)$$

the relation $(1/\lambda)_{s,p+1}=(1/\lambda)_{s,p}+(1/\lambda)_{s,p-1}$ no longer holds because of the dispersion of the refractive index, whereas in linear phenomena and the third order nonlinear optical phenomena, this relation is valid.

Fig.4—1—2 shows the relation between the second harmonic intensity and the wave length with $l=l_c=\pi/\Delta k_0$ and $l_A=\tau l_B$. Here $\Delta k_0=4\pi(n_{20}-n_{10})/\lambda_0$. As usual, the intense peaks occur at $(m,n)=(F_{k-1},F_k)$. But their positions shift a lot. For example, in Fig.4—1—2, we can see three intense peaks occuring at $\lambda_{s,p}$, as indicated by τ^p. They are $\lambda_{1,2}=1.318\mu m$, $\lambda_{1,3}=1.115\mu m$ and $\lambda_{1,4}=0.960\mu m$. Obviously $(1/\lambda)_{1,4}\neq(1/\lambda)_{1,3}+(1/\lambda)_{1,2}$. So the spectrum of the second harmonic intensity in reciprocal space does not exhibit self-similarity.

Here another interesting phenomenon should be noted which is somewhat similar to the extinction phenomenon in solid state physics. In both Figs.(4—1—1) and (4—1—2), the mode (2,2) does not appear. As discussed above, after the fundamental light passing through the entire superlattice, the resultant second harmonic light can be viewed as composed of two parts with a phase difference of $\exp[i(\Delta k l+\pi)]$. When the two satisfy the condition $(\Delta k l+\pi)=(2j+1)\pi$ or

$$l=2j\frac{\pi}{\Delta k}\ ,\ j=1,\ 2,\ 3,\ \ldots, \qquad (4\text{—}1\text{—}16)$$

they interfere destructively. Here $\pi/\Delta k$ is the coherence length for SHG. That is to say, when the structure parameter l equals an even number times the coherence length, the corresponding SHG will disappear. This can be also deduced from Eq.(4—1—8) easily. In Eq.(4—1—8), for mode (2,2), we can obtain $\Delta k l=2\pi$ from the δ-function. But then the factor $\sin(\Delta k l/2)=0$. So the second harmonic intensity is zero. By substituting for Δkl from Eq.(4—1—16) into the δ-function in Eq.(4—1—8), we can obtain the general extinction rule which is

$$(m,n)=(2j,2j). \qquad (4—1—17)$$

Namely, all peaks with their index (m,n)=(2j,2j) are absent in the spectrum of the second harmonic intensity.

§4—1—3.Summary

We have studied the second harmonic generation in the FOS theoretically. In our system, we find that because of the dispersive effect of the refractive index, the spectrum of the second harmonic intensity in reciprocal space does not reflect the symmetry of the quasiperiodic structure and thus does not exhibit self-similarity. Also found is the extinction phenomenon provided the structure parameters are properly selected. The general extinction rule has been obtained.

References of part 1:

1.F.Nori, and J.P.Rodriguez, Phys.Rev.B34,2207 (1986).

2.S.Tamura and J.P.Wolfe, Phys.Rev.B36, 3491 (1987).

3.Y.Y.Zhu, N.B.Ming and W.H.Jiang, Phys.Rev.B40, 8536 (1989).

4.R.Merlin, K.Bajema, R.Clarke, F.Y.Juang and P.K.Bhattacharya, Phys.Rev.Lett.55, 1768 (1985).

5.X.K.Zhang, H.Xia, G.X.Cheng, A.Hu and D.Feng, Phys.Lett.A136, 312 (1989).

6.Y.Y.Zhu, and N.B.Ming, Phys.Rev.B42, 3676 (1990).

7.J.Feng, Y.Y.Zhu, and N.B.Ming, Phys.Rev.B41, 5578 (1990).

8.J.P.Lu, T.Odagaki, and J.L.Birman, Phys.Rev.B33, 4809 (1986).

9.M.Kohmoto, and J.R.Banavar, Phys.Rev.B34, 563 (1986).

10.H.R.Ma, and C.H.Tsai, Phys.Rev.B35, 9295 (1987).

11.J.A.Armstrong, N.Bloembergen, J.Ducuing and P.S.Pershan, Phys.Rev.127, 1918 (1962).

12.N.Bloembergen, and A.J.Sievers, Appl.Phys.Lett.17, 483 (1970).

13.A.Yariv and P.Yeh,Optical waves in crystals (John Wiley $ sons, New York, 1984).

14.F.Zernike and J.M.Midwinter, Applied nonlinear optics (John Wiley &Sons, New York, 1973).

15.D.Levine and P.J.Steinhardt, Phys.Rev.B34, 596 (1986).

16.R.K.P.Zia and W.J.Dallas, J.Phys.A18, L341 (1985).

17.Smith, Opt.Commun.17, 332 (1976).

PART 2

Harmonic generations and the quasi-phase-matching[1]

The quasiperiodic superlattice has been studied a lot in recent years both theoretically and experimentally. Although there are suggestions[2,3] that the quasiperiodic superlattice can be of some practical usage, to our knowledge, the papers concerning this problem directly are still lack. In this part, we will propose a scheme by which a third harmonic can be generated in the Fibonacci optic superlattice(FOS) through the nonlinear optical effect. Compared with that generated by a conventional method, the intensity of the third harmonic generated here is a little larger. However, there are many other types of quasiperiodic superlattices[4—7], so it is hopeful that a much more effective superlattice for the generation of the third harmonic may be found.

§4—2—1.Theory

Here we consider a case in which a single laser beam with $\omega_1=\omega$ is incident from the left onto the surface of an FOS and through the nonlinear optical effect, the SHG and the third-harmonic generation(THG) exist simultaneously in the FOS. The configuration of the structure and the polarization states of the light waves are as those in part 1. Here, three optical fields must be taken into account, one for $\omega_1=\omega$, one for $\omega_2=2\omega$ and one for $\omega_3=3\omega$. The three optical fields, described in terms of their electric field components, are given by

$$E_i(x,t)=E_i(x)e^{i(\omega_i t-k_i x)},\ i=1,2,3, \qquad (4—2—1)$$

which satisfy the wave equation[8]

$$\nabla^2\vec{E}-\frac{\varepsilon_3}{c^2}\frac{\partial^2\vec{E}}{\partial t^2}=\frac{4\pi}{c^2}\frac{\partial^2\vec{P}}{\partial t^2}. \qquad (4—2—2)$$

The presence of these electric fields can give rise to nonlinear polarizations at frequencies ω_2 and ω_3 etc., which are

$$P_{2\omega}(x,t)=2d_{33}f(x)E_1^2(x)e^{i(2\omega_1 t-2k_1 x)},$$

$$P_{3\omega}(x,t)=4d_{33}f(x)E_1(x)E_2(x)e^{i[(\omega_1+\omega_2)t-(k_1+k_2)x]}. \qquad (4—2—3)$$

Before going into detailed analysis,we must make some assumptions. We assume that the variation of the field amplitudes with x is small enough so that $k_i dE_i/dx>>d^2E_i/dx^2$ and that the amount of power lost from the input beam (ω_1) is negligible, i.e., $dE_1(x)/dx=0$. We also assume that $E_1>>E_2$, E_3, this is the so called small signal approximation.

Under these conditions, using equations (4—2—1) — (4—2—3) and carrying out the indicated differentiation, we can get[8]

$$\frac{dE_1(x)}{dx}=0, \qquad (4—2—4a)$$

$$\frac{dE_2(x)}{dx} = -i\frac{16\pi\omega^2}{k^{2\omega}c^2} d_{33} f(x) E_1^2 e^{i(k^{2\omega}-2k^{\omega})x} , \qquad (4\text{—}2\text{—}4b)$$

$$\frac{dE_3(x)}{dx} = -i\frac{72\pi\omega^2}{k^{3\omega}c^2} d_{33} f(x) E_1 E_2(x) e^{i(k^{3\omega}-k^{2\omega}-k^{\omega})x} . \qquad (4\text{—}2\text{—}4c)$$

In equations (4—2—4) only the largest terms have been kept.

By integrating the equations (4—2—4), the electric fields after passing through a general block can be represented as

$$E_1(x_j) = E_1(0), \qquad (4\text{—}2\text{—}5a)$$

$$E_2(x_j) = E_2(x_{j-1}) + \frac{1}{4} K_1 (1-2e^{i\Delta k l} + e^{i\Delta k L'}) e^{i\Delta k x_{j-1}} E_1^2 , \qquad (4\text{—}2\text{—}5b)$$

$$E_3(x_j) = E_3(x_{j-1}) + \frac{1}{4}\frac{K_2}{K_1} E_1 (1-2e^{i\Delta k' l} + e^{i\Delta k' L'}) e^{i\Delta k' x_{j-1}} E_2(x_{j-1})$$

$$+\frac{1}{16} K_2 \left\{ 1+(1-2e^{i\Delta k l})(e^{i\Delta k' L'} - e^{i\Delta k' l}) - e^{i\Delta k' l} \right\} e^{i(\Delta k+\Delta k')x_{j-1}} E_1^3$$

$$+\frac{1}{16} K_2 \frac{\Delta k'}{(\Delta k+\Delta k')} \left\{ e^{i(\Delta k+\Delta k')L'} - 1 \right\} e^{i(\Delta k+\Delta k')x_{j-1}} E_1^3 \qquad (4\text{—}2\text{—}5c)$$

Where

$$\Delta k = k^{2\omega} - 2k^{\omega},$$

$$\Delta k' = k^{3\omega} - k^{2\omega} - k^{\omega} ,$$

$$K_1 = \frac{64\pi\omega^2}{k^{2\omega} c^2 \Delta k} d_{33} ,$$

$$K_2 = \frac{288\pi\omega^2}{k^{3\omega} c^2 \Delta k'} d_{33} K_1 , \qquad (4—2—6)$$

and x_j is the position of the second interface of the jth block as shown in Fig.1—3. When $L' = l_A = l_{A1} + l_{A2}$, the equations are for blocks A, when $L' = l_B = l_{B1} + l_{B2}$, they are for blocks B. In deriving Eqs.(4—2—5), the boundary conditions have been used which are $E_1(0) = E_1$, $E_2(0) = 0$, $E_3(0) = 0$.

THe equations (4—2—5) can be written in a matrix form

$$\begin{pmatrix} E_1^3(x_j) \\ E_2(x_j) \\ E_3(x_j) \end{pmatrix} = T^{A(B)} \begin{pmatrix} E_1^3(x_{j-1}) \\ E_2(x_{j-1}) \\ E_3(x_{j-1}) \end{pmatrix} , \qquad (4—2—7)$$

where

$$T^{A(B)} = \begin{pmatrix} 1 & 0 & 0 \\ T_{21}^{A(B)} & 1 & 0 \\ T_{31}^{A(B)} & T_{32}^{A(B)} & 1 \end{pmatrix} , \qquad (4—2—8)$$

with

$$T_{21}^{A(B)} = \frac{1}{4} K_1 \left\{ 1 - 2e^{i\Delta k l} + e^{i\Delta k l_{A(B)}} \right\} e^{i\Delta k x_{j-1}} ,$$

$$T_{31}^{A(B)}=\frac{1}{16}K_2\left\{1+(1-2e^{i\Delta k l})(e^{i\Delta k' l_{A(B)}}-e^{i\Delta k' l})-e^{i\Delta k' l}\right\}$$

$$\times e^{i(\Delta k+\Delta k')x_{j-1}}+\frac{1}{16}K_2\frac{\Delta k'}{(\Delta k+\Delta k')}\left\{e^{i(\Delta k+\Delta k')l_{A(B)}}-1\right\}$$

$$\times e^{i(\Delta k+\Delta k')x_{j-1}},$$

$$T_{32}^{A(B)}=\frac{1}{4}\frac{K_2}{K_1}E_1(1-2e^{i\Delta k' l}+e^{i\Delta k' l_{A(B)}})e^{i\Delta k' x_{j-1}}. \qquad (4—2—9)$$

Thus the output electric fields after passing through N blocks are

$$\begin{pmatrix}E_1^3(x_N)\\E_2(x_N)\\E_3(x_N)\end{pmatrix}=T^N\begin{pmatrix}E_1^3\\0\\0\end{pmatrix}, \qquad (4—2—10)$$

where $T^N=\ldots T^A T^B T^A T^B T^A T^A T^B T^A$, i.e., T^N is the product of N matrices.

These equations constitute the basis of our numerical calculations and discussions of this paper. We will discuss them in detail in the following section.

§4—2—2. Numerical calculations and discussions

We have performed numerical computations for both SHG and THG with the pump beam at wave length 1.318μm of Nd:YAG laser. For $LiNbO_3$ crystals, under room temperature, the refractive indices, according to the Hobden and Warner's

equation[9], are

n_o=2.2215, n_e=2.1436 at λ=1.318μm,

n_o=2.2839, n_e=2.1953 at λ=0.659μm,

n_o=2.3913, n_e=2.2882 at λ=0.439μm.

A.Second harmonic generation(SHG)

The SHG is the result of two intense pump beam mixing. Under the condition of small signal approximation,the second harmonic intensity depends completely on the structures of the superlattice, i.e., depends on whether it is quasi-phase-matched or not.

In a homogeneous medium, the term $\sin(\frac{1}{2}\Delta kx/\Delta k)$ is crucial to the success of the experiment[8]. To obtain a significant amount of power, it is obviously necessary to achieve a condition where

$$\Delta k=k^{2\omega}-2k^{\omega}=0 \qquad (4\text{—}2\text{—}11)$$

is fulfilled. This is called the phase matching condition. For a periodic structure, a similar term exists which is $\sin[\frac{1}{2}(\Delta k-G_m)x/(\Delta k-G_m)]$(see Eq.4—1—9). The condition

$$k^{2\omega}-2k^{\omega}-G_m=0 \qquad (4\text{—}2\text{—}12)$$

is the so-called quasi-phase-matching which was predicted theoretically by Bloembergen et al.[10,11] at 1962 and proved experimentally by several groups[12-15]. Likewise, for a quasiperiodic structure, we can also define a quasi-phase-matching condition because of the resemblance of

Eqs.(4—1—7) and (4—1—9), which is

$$k^{2\omega}-2k^{\omega}-G_{m,n}=0. \qquad (4—2—13)$$

The meaning of these conditions are almost the same. When they are satisfied, the output of the SHG will be strong; when not, the output will be very weak.

Fig.4—2—1 shows the relationship between the second harmonic intensity and the block number with $l=l_c^{2\omega}=\pi/(k^{2\omega}-2k^{\omega})$, $t=\tau$ and η taking various values. Note that when $\eta=0$, the enhancement of the second harmonic intensity is proportional to the square of the block number as curve(A) of Fig.4—2—1 indicates. It is just the result of a periodic one. For when $\eta=0$, the FOS turns back to a periodic optic superlattice(see Eq.1—12) and $l=l_c^{2\omega}=\pi/(k^{2\omega}-2k^{\omega})$ is just the quasi-phase-matching condition. The curves (B) and (C) represent the enhancement of the second harmonic intensity with $\eta=0.15$ and $\eta=0.30$. The curve of $\eta=0.15$ grows more slowly than the square dependence curve (A), but more rapidly than the curve of $\eta=0.30$. It should be mentioned that, in our choice of the structure parameters, no matter what values η takes, the condition $l=\pi/(k^{2\omega}-2k^{\omega})$ is equivalent to $k^{2\omega}-2k^{\omega}-G_{1,1}=0$, the quasi-phase-matching.

Fig.4—2—2 shows the relationship between the second harmonic intensity and the block number with $k^{2\omega}-2k^{\omega}-G_{m,n}\neq 0$. Obviously, the SHG is very inefficient.

Comparing Eqs.(4—2—13) with (4—2—12), we find that it is the reciprocal vector the structures provide which

compensates the dispersion of the refractive index and makes the nonlinear optic process phase matched.

B.Third harmonic generation(THG)

The process of the THG discussed here is a coupled parametric process, that is, two parametric processes, the SHG process and the frequency upconversion process(FUP) which mixes the fundamental frequency with the second harmonic, are coupled in this material.

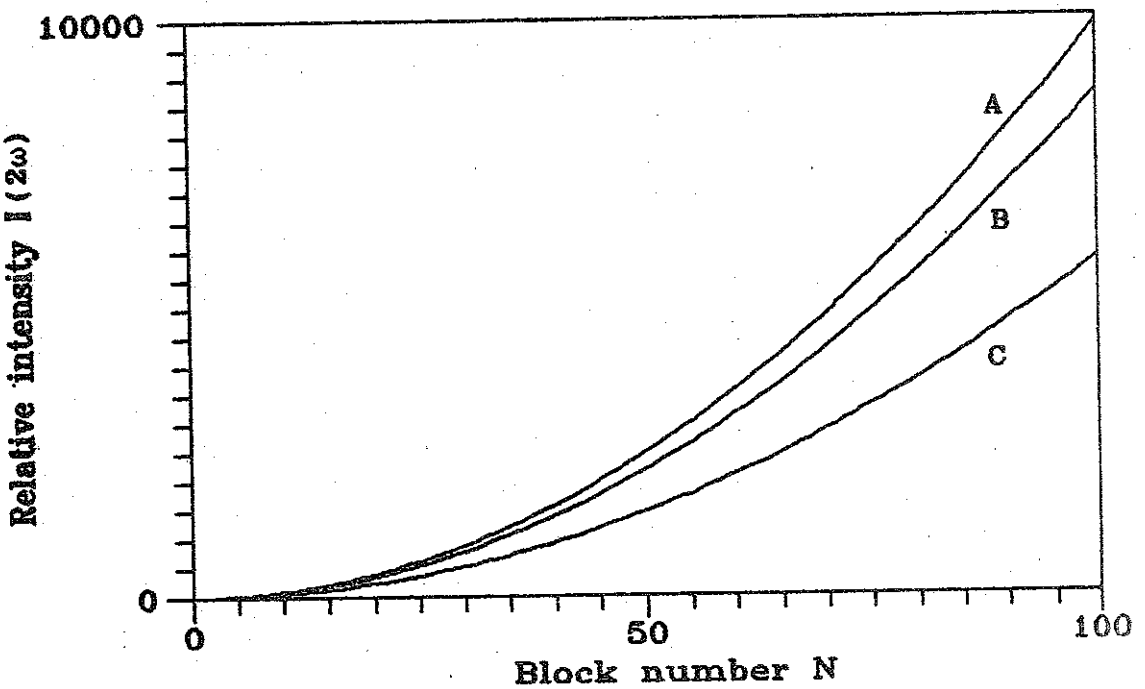

Fig 4—2—1.The dependence of the second harmonic intensity on the block number with l=6.37μm in different cases. (A)η=0, i.e., in a periodic optic superlattice; (B)η=0.15, i.e., in a Fibonacci optic superlattice; (C)the same as (B) with η=0.30. For both (B) and (C), $k^{2\omega}-2k^{\omega}-G_{m,n}=0$.

According to Eq.(1—12), three parameters (l,η,t) are

adjustable. We have calculated the relationship between the third harmonic intensity and these parameters separately.

Fig.4—2—3 shows the dependence of the third-harmonic intensity on l with N=100, η=-0.02 and t=1.62. Clearly, there exist three maximum values in the range of l=5.90μm to l=6.40μm. They occur at (1)l_1=5.98μm; (2)l_2=6.08μm; (3)l_3=6.37μm.

Fig.4—2—4 shows its dependence on η with N=100 while

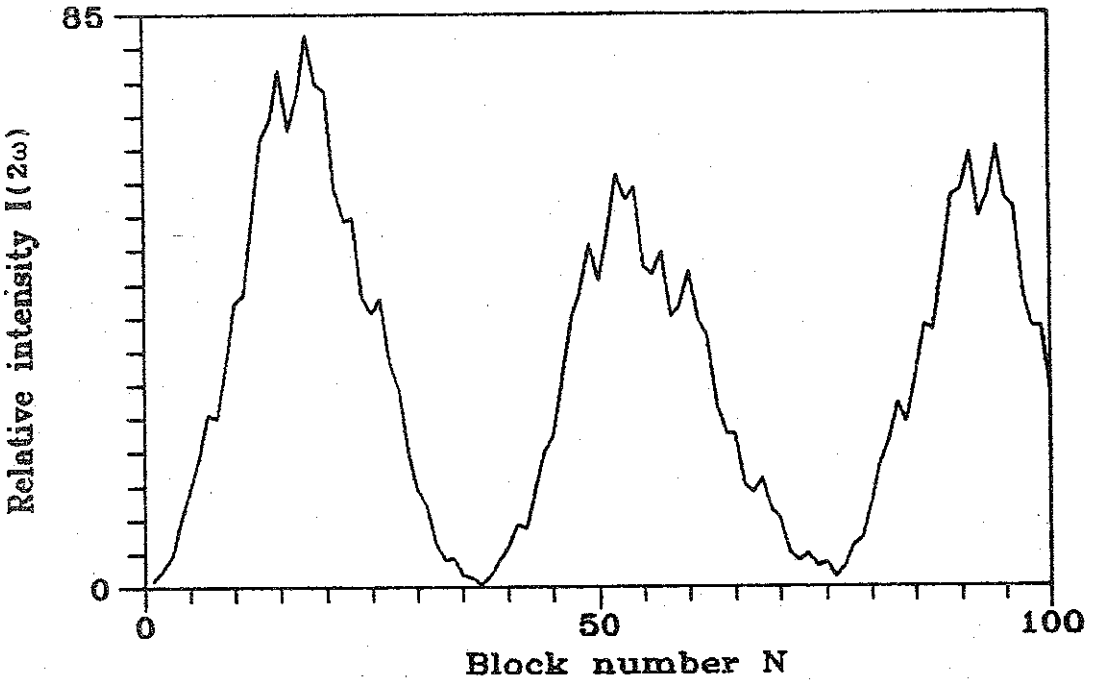

Fig.4—2—2.The dependence of the second harmonic intensity on the block number with $k^{2\omega}-2k^{\omega}-G_{m,n}\neq 0$.

l takes these three values separately. We find that for each value of l, there is an optimum value of η where the intensity reaches its maximum. By repeated adjustment of these parameters, an optimum condition has been found which is l=6.08μm, η=0.01, t=1.90 with the third harmonic

intensity $I_{3\omega}=122000K_2^2$ (Fig.4—2—5, curve(C)). Below we will discuss some interesting phenomena.

Taking $l=l_c^{2\omega}=\pi/\Delta k$, ($l_c^{2\omega}=6.37\mu m$) and $l=5.98\mu m$, we have calculated the dependence of the third harmonic intensity on the block number which is shown in Fig.4—2—5. The two curves differ from each other in nature completely, one fluctuates drastically while the other increases steadily with the block number. The explanation is as follows.

As discussed above, when $l=l_c^{2\omega}=6.37\mu m$, the second harmonic is quasi-phase-matched and its intensity increases with the block number as Fig.4—2—1 shows. But then, the third harmonic is not quasi-phase-matched. In some parts of the superlattice, the third harmonic is constructive, in some other parts of the superlattice, it is destructive. So

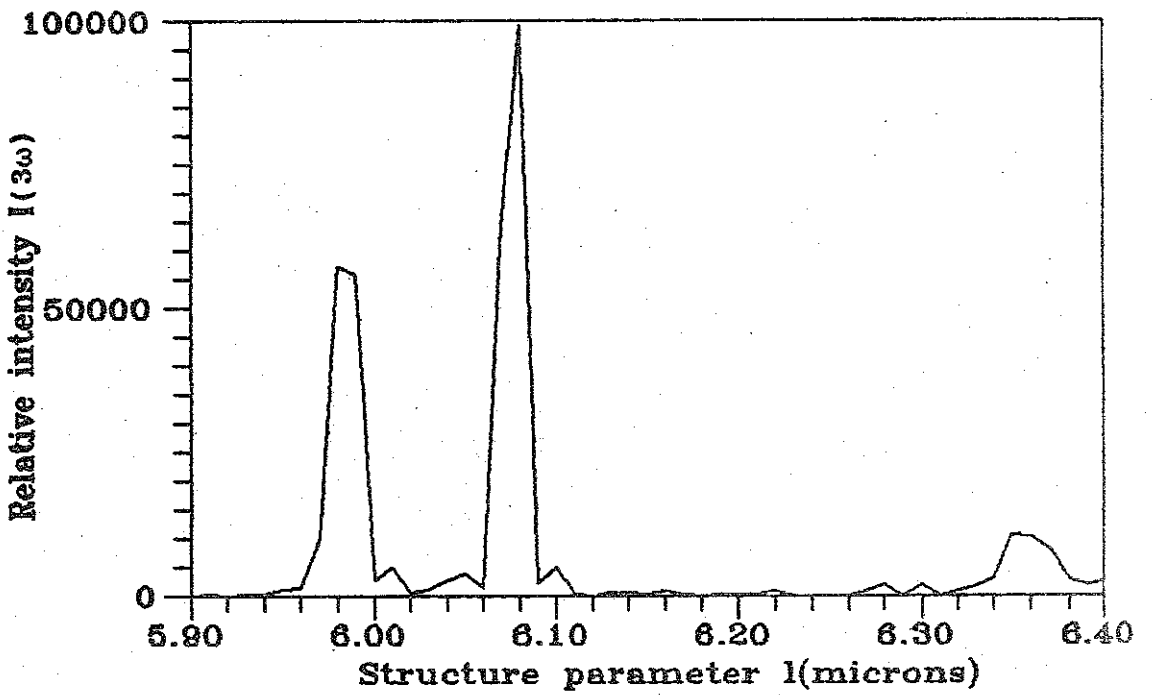

Fig.4—2—3.The dependence of the third harmonic intensity on l with N=100, η=-0.02 and t=1.62.

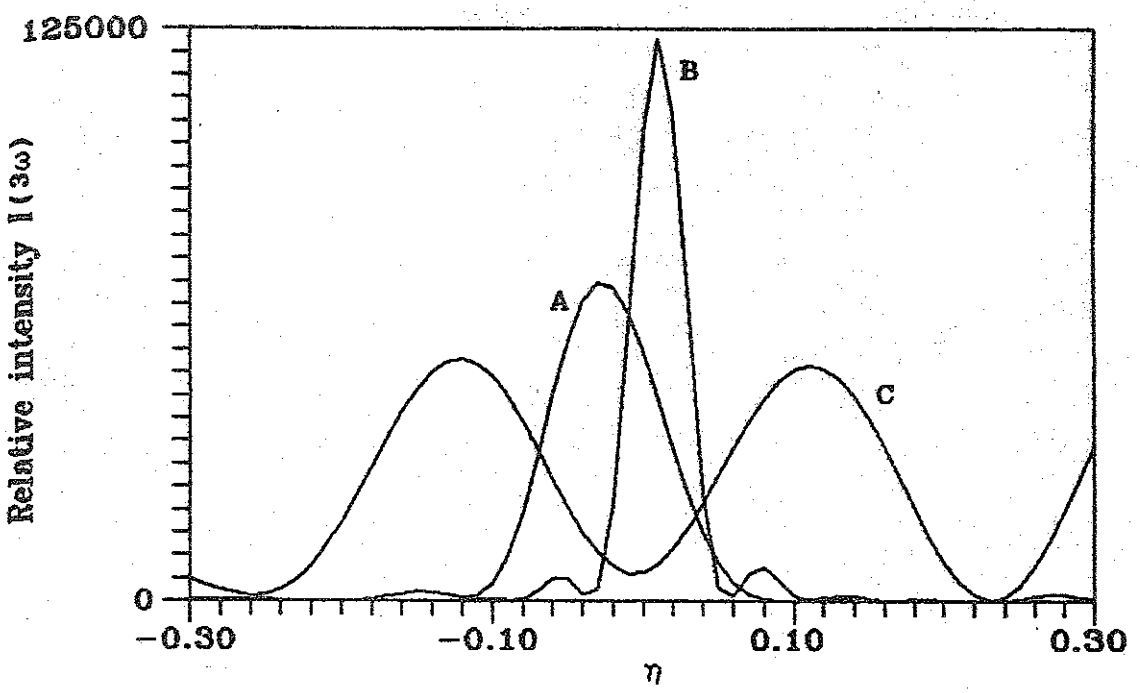

Fig.4—2—4.The dependence of the third harmonic intensity on η with N=100.(A)l=5.98μm; (B)l=6.08μm; (C)l=6.37μm.

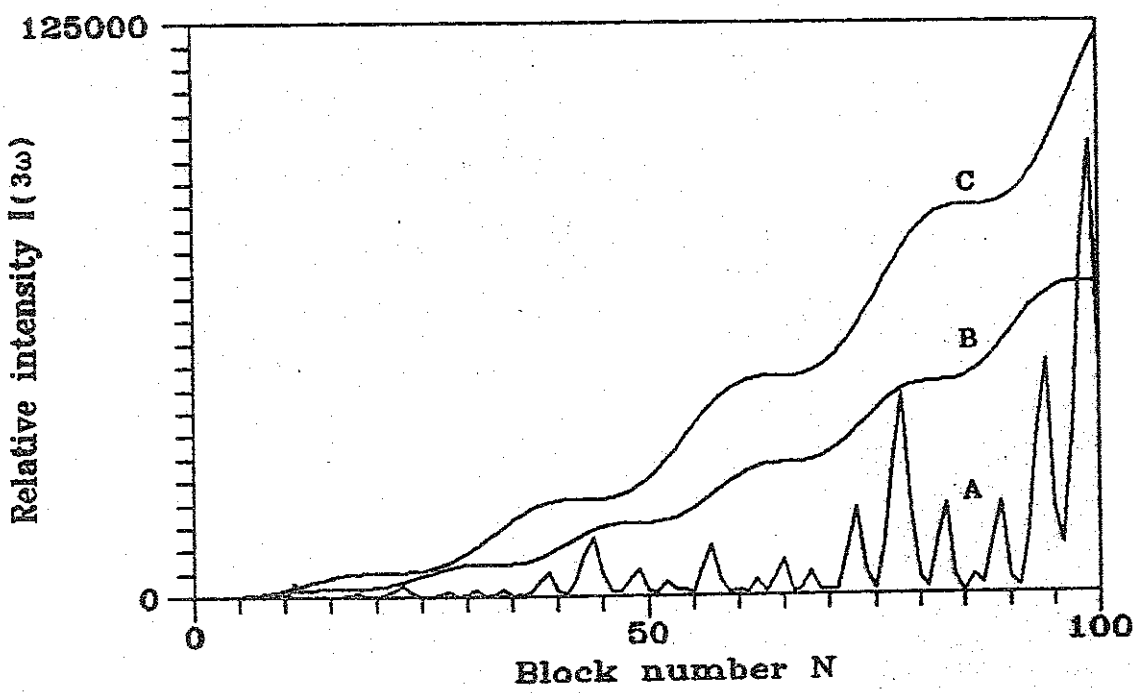

Fig.4—2—5.The dependence of the third harmonic intensity

on the block number under different conditions.(A) l=6.37μm, η=-0.10, t=1.62; (B) l=5.98μm, η=-0.02, t=1.78; (C) l=6.08μm, η=0.01, t=1.90.

its intensity fluctuates drastically as the block number varies. Fig.4—2—5(A) shows this feature clearly. But from Eqs.(4—2—5), we can see that the THG depends not only on the structure parameters but also on the second harmonic intensity. So as the block number increases, the third harmonic intensity undulates more severely while the second harmonic intensity increases steadily.

When l=5.98μm, we find that

$$\Delta k' l = 3\pi. \qquad (4—2—14)$$

Therefore, $l=3l_c^{3\omega}$, here $l_c^{3\omega}$ represents the coherent length for the THG in a single FUP. Why l should take the value three times the $l_c^{3\omega}$ is obvious. Because if $l=l_c^{3\omega}$, the THG in a single FUP is quasi-phase-matched, but the SHG is phase mismatched severely. The result is that the generated THG is very inefficient because of its relation to the SHG. We know that, as far as the phase factor is concerned, the effect of $l=3l_c^{3\omega}$ is the same as the effect of $l=l_c^{3\omega}$ for THG. And when $l=3l_c^{3\omega}$, the mismatch of the SHG becomes smaller. Thus the third harmonic intensity increases with the block number(Fig.4—2—5, curve(B)).

The curves 4—2—5(B) and 5(C) resemble each other. They are of the shape of step-like. In both cases, the second harmonic are phase-mismatched. Fig.4—2—6 reveals

this feature. The second harmonic intensity fluctuates almost sinusoidally. There is a one-to-one correspondence between Figs.4—2—6 and 4—2—5. Whenever the second harmonic intensity decreases, a platform appears on the third harmonic intensity. And more, since the maximum value of the second harmonic intensity in Fig.4—2—6(A) is much larger than that in 6(B), its corresponding third harmonic intensity is much stronger. This strongly indicates the dependence of the THG on the SHG.

To obtain an appreciation for the enhancement of the third harmonic available in our case, consider a commonly used two step process[16]. The SHG is generated in the first $LiNbO_3$ crystal of 100 $I_c^{2\omega}$ long using nonlinear coefficient

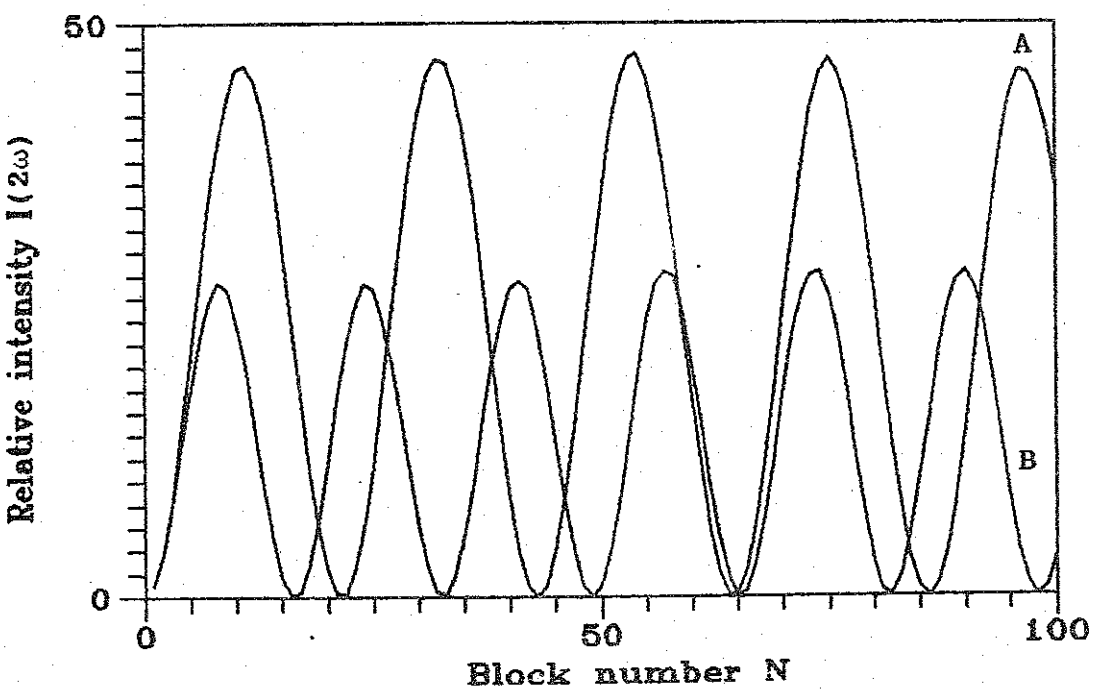

Fig.4—2—6.The dependence of the second harmonic intensity on the block number. (A) l=6.08μm, η=0.01, t=1.90; (B) l=5.98μm, η=-0.02, t=1.78.

d_{31} with the phase-matched, then it mixes with the fundamental frequency in the second $LiNbO_3$ crystal of $100\times 3l_c^{3\omega}$ long using the same nonlinear coefficient, here $l_c^{3\omega}=\pi/\Delta k'$, the relative output intensity of the THG is $I=99000K_2^2$. We find that the third harmonic intensity in our case is fairly well though not so exciting. However, since there are many other types of quasiperiodic superlattices, it may be possible to find one in which SHG and THG can be phase-matched simultaneously. In that case, the THG can be generated much more efficiently, which is favorable to the practical applications.

§4—2—3.Summary

We have presented a detailed theoretical analysis of the SHG and THG in the FOS. A particular technique has been proposed which is the first direct depiction of the practical applications of quasiperiodic superlattices, although the results are not so exciting.

The analysis used here can be carried over to many other types of quasiperiodic superlattices and to the Fibonacci superlattices of other materials. To deal with quasiperiodic superlattices consisting of different materials with different refractive indices along the optical propagation direction, the reflection by the interfaces must be considered.

The FOS discussed here is a new solution to the quasi-phase-matching of the optical parametric processes. With this material, not only might the SHG and the THG have applicable enhancement, but also other parametric processes

might proceed with large enhancement.

References of part 2:

1.J.Feng, Y.Y.Zhu, and N.B.Ming, Phys.Rev.B41, 5578 (1990).

2.L.Macon, J.P.Desideri, and D.Sornette, Phys.Rev.B40, 3605 (1989).

3.C.Schwartz, Appl.Opt.27, 1232 (1988).

4.J.P.Lu, T.Odagaki, and J.L.Birman, Phys.Rev.B33, 4809 (1986).

5.G.Gumbs, and M.K.Ali, Phys.Rev.Lett.60, 1081 (1988).

6.J.Birch, M.Severin, U.Wahlstrom, Y.Yamamoto, G.Radnoczi, R.Riklund, J.E.Sundgren, and L.R.Wallenberg, Phys.Rev.B41, 10398 (1990).

7.M.Dulea, M.Severin, and R.Riklund, Phys.Rev.B42, 3680 (1990)

8.F.Zernike and J.M.Midwinter, Applied nonlinear optics (John Wiley $ Sons, New York, 1973).

9.M.V.Hobden and J.Warner, Phys.Lett.22, 243 (1966).

10.J.A.Armstrong, N.Bloembergen, J.Ducuing and P.S.Pershan, Phys.Rev.127, 1918 (1962).

11.N.Bloembergen and A.J.Sievers, Appl.Phys.Lett.17, 483 (1970).

12.D.Feng, N.B.Ming, J.F.Hong, Y.S.Yang, J.S.Zhu, Z.Yang and Y.N.Wang, Appl.Phys.Lett.37, 607 (1980).

13.Y.H.Xue, N.B.Ming, J.S.Zhu and D.Feng, Chinese Phys.4, 554 (1984).

14.A.Feisst, and P.Koidl, Appl.Phys.Lett.47, 1125 (1985).

15.G.A.Magel, M.M.Fejer, and R.L.Byer, Appl.Phys.Lett.56, 108 (1990).

16.R.Piston, Laser Focus 14, 66 (1978)

PART 3

More rigorous treatment of the SHG

The conventional method of treating the second harmonic generation involves two assumptions, the first is the small signal approximation and the second is the parabolic approximation which neglects the second-order derivative in the wave equation. We have known that the small signal approximation is equivalent to the kinematical theory of diffraction in x-ray or electron and leads to the breakdown of the energy conservation. In order to see the effect of the second approximation on the SHG, here in this part we will solve the problem more strictly. Only the first assumption is remained, the second one is removed.

Here we start from Eq.(4—1—2). Its solution can be obtained through two steps. First we solve the corresponding homogeneous equation

$$\frac{\partial^2 E_2}{\partial x^2} - 2ik^{2\omega}\frac{\partial E_2}{\partial x} = 0. \qquad (4—3—1)$$

Its solution is

$$E_{20} = C_1 + C_2 e^{i2k^{2\omega}x} . \qquad (4—3—2)$$

Next, we use the method of variation of constants to obtain the solution of Eq.(4—1—2), which is

$$E_2=C_1(x)+C_2(x)e^{i2k^{2\omega}x}. \qquad (4\text{—}3\text{—}3)$$

Through the conventional procedures, we have

$$\frac{\partial C_1}{\partial x}=-i\frac{16\pi\omega^2}{k^{2\omega}c^2}d_{33}f(x)E_1^2e^{i(k^{2\omega}-2k^{\omega})x}, \qquad (4\text{—}3\text{—}4)$$

$$\frac{\partial C_2}{\partial x}=i\frac{16\pi\omega^2}{k^{2\omega}c^2}d_{33}f(x)E_1^2e^{-i(k^{2\omega}+2k^{\omega})x}. \qquad (4\text{—}3\text{—}5)$$

The solution of Eq.(4—3—4) describes a forward-going second harmonic wave and the solution of Eq.(4—3—5) describes a backward-going one. For a given structure, only one kind of wave can be enhanced efficiently, either the forward-going one or the backward-going one. Since we have already discussed the former one, so here we will merely study the latter one. The solution of Eq.(4—3—5) is

$$E_2^{back}(\Delta k,t)=i\frac{32\pi\omega^2}{k^{2\omega}c^2}d_{33}E_1^2\sum_{m,n}e^{-i(\frac{1}{2}G_{m,n}l-X_{m,n})}\frac{\sin\frac{1}{2}G_{m,n}l}{\frac{1}{2}G_{m,n}}$$

$$\times\frac{\sin X_{m,n}}{X_{m,n}}\delta(K-G_{m,n})e^{i(2\omega t+k^{2\omega}x)}, \qquad (4\text{—}3\text{—}6)$$

here $K=k^{2\omega}+2k^{\omega}$, other notations are as before.

Obviously, in any case, K can not be equal to zero, hence the backward-going second harmonic can never be phase matched in a homogeneous medium. It is reasonable to neglect

the second-order derivative in Eq.(4—1—2), which results in the disappearance of the backward-going second harmonic. But in a periodic or a quasiperiodic structure, the phase mismatch of the SHG process can be compensated with the reciprocal vectors the structure provides. Therefore the backward-going second harmonic can be quasi-phase-matched and enhanced enormously. This new phenomenon may have some applications in future.

Likewise, starting from Eq.(4—3—6), we can discuss the spectrum of the backward-going second harmonic and the dispersive effect of the refractive index on the spectrum as well as the extinction phenomenon. The results are much the same as those of the forward-going second harmonic.

CHAPTER 5

Electrooptic effect and transmission spectrum of light in Fibonacci optic superlattice

Ordinarily, the propagation of lights in a dielectric medium only relates to the dielectric tensor, a second-rank one. In chapter 1, we have already proved that the dielectric tensor is the same in positive domains and negative domains for a crystal with its symmetry of 3m point group. So the optic superlattice will be homogeneous to the propagation of lights. But this is valid only in the absence of an external electricn field. For electrooptic crystals, $LiNbO_3$ being one of them, the dielectric tensor can be modulated by an external electric field[1]. Since the positive domain and negative domain act differently to the electric field, the dielectric tensor is no longer the same in these two types of domains. The electric field can be applied onto the media through more than one scheme[1]. For example, for FOS of $LiNbO_3$ crystals as shown in Fig.1—3, if the applied electric field is along the z axis, then only the diagonal elements of the dielectric tensor is affected. In this case, the light will be reflected by the interfaces with its polarization unchanged. If, on the other hand, the applied electric field is along the y axis (or x axis), then only the off-diagonal elements of the dielectric tensor is affected, at least in the first order approximation. In this case, the energy of lights with different polarizations will be coupled together. In this chapter, only the latter one